

The influence of initial morphology of one-way drawn poly(ethylene terephthalate) films on their transverse drawing

J. B. Faisant de Champchesnel and J. F. Tassin

*Université du Maine, Laboratoire de Physicochimie Macromoléculaire,
URA CNRS No. 509, Avenue Olivier Messiaen, BP 535, 72017 Le Mans Cedex, France*

and D. I. Bower and I. M. Ward*

University of Leeds, IRC in Polymer Science and Technology, Leeds LS2 9JT, UK

and G. Lorentz

*Rhône-Poulenc Films, Magphane International, Saint Maurice de Beynost, BP 140,
01701 Miribel Cedex, France*

(Received 22 November 1993; revised 14 March 1994)

A study of the development of molecular orientation and crystalline structure during the transverse drawing of one-way drawn poly(ethylene terephthalate) films has been carried out. The influence of the size of the crystallites in the one-way drawn film and the influence of the transverse drawing temperature have been studied. It is shown that the deformation mechanisms appear to depend on the size of the crystals initially present. Films containing small crystals lead to a higher orientation and larger crystalline structures oriented along the transverse direction. The influence of the second drawing temperature can be understood as a result of the importance of molecular relaxation and crystallization, both of which are enhanced by elevated temperatures.

(Keywords: poly(ethylene terephthalate); drawn films; morphology)

INTRODUCTION

Improvement of the mechanical properties and quality of sequentially biaxially stretched poly(ethylene terephthalate) (PET) films requires knowledge at a molecular level of the chain deformation processes and the development of structure during the industrial process.

Previous studies in our group have dealt with the uniaxial planar drawing process, and the influence of macroscopic parameters (temperature, strain rate, draw ratio) has been analysed using spectroscopic techniques¹⁻⁴. The setting up of a specially designed stretching machine has allowed us to study the main processes involved in the transverse drawing under well defined conditions⁵. However, it is known from film manufacturers that the film drawability during this second step is highly dependent on the structure of the initial one-way drawn film.

To obtain a better understanding of this observation, an extensive study of the influence of the initial structure on the orientation processes during transverse stretching has been carried out. Since many parameters are responsible for the structure of the one-way drawn films, it was decided to study the second drawing step, not systematically as a function of the various parameters of the first stretching, but as a function of the differences in

structure shown by the initial one-way drawn films. More precisely, owing to orientation-induced crystallization, the morphology of the one-way drawn films involves either long or short, or thin or thick, crystalline blocks.

In the first part of this paper, the influence of the film structure before the second drawing will be studied. The influence of the second drawing temperature will be described in the second part. In each part, the experimental results for the crystalline phase will be reported and a brief discussion will be given of the overall orientation (in both crystalline and amorphous phases) of the normals to the phenylene rings. A final discussion will summarize the main features of this study.

MATERIALS

Choice of the one-way drawn films

The crystalline structure in the initial one-way drawn film can be controlled by temperature, draw ratio and type of stretching. In the particular case of amorphous PET films drawn at constant width under a constant drawing force, the main feature of the process is that, for a given force and temperature, the draw ratio reaches a maximum value, which corresponds to the equilibrium of a molecular crystalline network under a given stress. The kinetics of the longitudinal deformation process are such that the final desired draw ratio can be reached in

* To whom correspondence should be addressed

Table 1 Characteristics of one-way drawn films

Kind of sample	First drawing temperature, T_1 (°C)	First draw ratio, λ_1	Maximum strain rate, $\dot{\epsilon}_{\max}$ (s^{-1})	Thickness (μm)	Crystallinity (%)
Quenched:	100	3.2	4.19	50	8.6
small	103	3.4	–	47	8.6
crystallites	105	3.2	3.27	50	7.2
Equilibrium:	100	3.9	8.45	41	25.2
large	105	3.6	16.73	44	29.5
crystallites	125	3.4	10.28	47	28.0

two quite different ways^{6,7}. The sample at the final draw ratio can be either 'at equilibrium' or 'quenched', depending on whether the sample has reached the equilibrium deformation under the applied conditions of load and temperature, or the deformation process has been mechanically stopped before reaching this equilibrium state. The crystalline structure of the one-way drawn films is highly dependent on the drawing process. For example, the crystallite size decreases as the temperature or draw ratio is decreased⁸.

The one-way drawn films used throughout this study have been obtained on a pilot plant. On the pilot plant, the draw ratios are fixed by the ratio of the speeds of the fast rolls and slow rolls, whereas the drawing force is directly related to the absolute roll speed. Temperature is estimated from the film surface temperature measured using an infra-red camera. Different crystalline structures can be obtained by choosing to produce 'equilibrium' or 'quenched' films under various temperature conditions.

One-way drawn samples containing small crystals are 'quenched' samples drawn at temperatures between 100 and 105°C, whereas those with large crystals are 'equilibrium' samples drawn at temperatures between 100 and 125°C. The characteristics of the one-way drawn samples are reported in *Table 1*. The drawing temperatures for the one-way drawn samples are only approximate but are correct relative to each other.

Transverse stretching of the one-way drawn samples

For the second draw, samples with dimensions $30 \times 100 \text{ mm}^2$ were cut from the one-way drawn samples and stretched transverse to the first drawing direction on a specially designed drawing machine at the Saint Fons Research Centre of Rhône-Poulenc⁵; the width normal to the second draw direction was kept constant at 100 mm.

It is impossible to bring the sample from ambient to the stretching temperature without to some extent modifying the structure of the one-way drawn material. In an attempt to minimize the modification, the following preheating programme was applied to each sample prior to stretching: 30 s heating at 87°C followed by 3 s heating at the second drawing temperature. During this preheating programme, the sample was held at constant width and constant length, i.e. it was totally constrained.

It was important to establish the state of the sample before the second drawing. In addition to the transversely stretched films, two samples were cut from each one-way drawn film: one to be analysed as it was and the other after having undergone the preheating cycle while totally constrained to check the effect of this preheating on the structure of the film.

For the study of the second drawing itself, samples were stretched at constant speed from 30 mm to either 60 or 90 mm long, corresponding to average draw ratios λ_2 of 2 and 3, respectively. The homogeneity of the film deformation was checked using a grid drawn on the sample prior to stretching, and slight differences were observed across the sample. Biaxially drawn samples showing variations in λ_2 higher than ± 0.3 were rejected. It must be pointed out that the transverse drawing of one-way drawn films that have reached the equilibrium state leads to less homogeneous films than does the transverse drawing of quenched one-way drawn films. In the figures presented in this paper, the draw ratios shown correspond to those measured on the grid and may differ slightly for the same film depending on the part of the film that was used when carrying out the particular measurement reported.

The linear drawing speed of the jaws was chosen so that the average initial strain rate $\dot{\epsilon}_{\text{initial}}$ remains the same for all the samples. This initial strain rate is the maximum strain rate at which the sample is deformed during the stretching. The drawing procedure was set to keep this strain rate at 0.25 s^{-1} . The drawing time is typically 4 s for $\lambda_2 = 2$ and 8 s for $\lambda_2 = 3$.

GENERAL THEORETICAL BACKGROUND

Description of orientation

Although the development of orientation can be shown graphically by pole figures, it is desirable to use quantitative measures of the orientation with respect to the principal directions of the film.

The quantities used to describe the orientations are the average values P_{200}^{iJ} of the second-order Legendre polynomial $P_2(\cos \theta)$, defined as:

$$P_{200}^{iJ} = \frac{1}{2} \langle 3 \cos^2 \theta_{iJ} - 1 \rangle$$

where i refers to a molecular direction, the orientation of which has to be characterized with respect to the principal axis J of the film; θ_{iJ} is the angle between molecular direction i and macroscopic direction J and the angle brackets denote an average over all molecular units. This average takes a value of 0 when the distribution of units is isotropic and 1 when all the units are aligned parallel to the reference axis with respect to which P_{200} is calculated.

Further quantitative measures of the orientation distribution function can be obtained by calculating higher-order averages⁹ such as P_{400}^{iJ} , the average of the fourth-order Legendre polynomial, which give additional information about the shape of the distribution.

Conventions

In the case of biaxial stretching, the macroscopic directions are the principal directions of the film. They will be referred to as the machine direction (MD) for the direction of the first longitudinal stretching (Ox_3), the transverse direction (TD) for the direction of the second transverse drawing (Ox_1) and the normal direction (ND) for the direction normal to the plane of the film (Ox_2).

EXPERIMENTAL

X-ray diffraction

Wide-angle X-ray diffraction has been used to characterize the distribution of orientations of various crystallographic directions as well as the crystalline dimensions along these directions.

To investigate the distribution of orientations, X-ray data were obtained for two reflections: $(\bar{1} 0 5)$ (plane normal close to the chain axis) and $(1 0 0)$ (plane normal close to the normal to the phenylene ring). A Huber wide-angle X-ray diffractometer was used. The measurement of orientation of these two crystallographic directions was undertaken using the experimental procedure described earlier⁵.

The crystalline sizes were obtained for three crystallographic directions: $(\bar{1} 0 5)$, $(1 0 0)$ and $(0 1 0)$; the last crystallographic direction is roughly perpendicular to the first two. The crystallite size along $[h k l]$ will be called L_{hkl} in the following sections. $L_{\bar{1}05}$ corresponds to the length of the crystallite, L_{100} to the thickness and L_{010} roughly to the width. Both the Huber wide-angle diffractometers of the Universities of Leeds (UK) and Le Mans (France) were used. Further experimental details can be found in ref. 5.

Refractive indices

The refractive indices of the samples were measured along the three principal directions using a BS-60 Abbe refractometer at the University of Leeds.

Density d and crystallinity χ were calculated from the mean refractive index $\bar{n} = (n_1 + n_2 + n_3)/3$ by the following formulae¹⁰:

$$d = 4.047 \left(\frac{\bar{n}^2 - 1}{\bar{n}^2 + 2} \right) \text{ g cm}^{-3}$$

$$\chi = \frac{d - d_a}{d_c - d_a}$$

where d_a is the density of the amorphous phase and d_c

is the density of the crystalline phase. These were taken to be 1.335 and 1.455 g cm⁻³ respectively¹¹.

Orientation of the normal to the phenylene ring

If $Ox_1x_2x_3$ is an orthogonal set of axes attached to the molecular unit of the PET chain, where Ox_3 is parallel to the chain axis and Ox_1 is perpendicular to Ox_3 and in the plane of the phenylene ring, Ox_2 will be close to the normal to the ring. If α_i is the molecular polarizability along Ox_i , it has been shown¹² that, to a good approximation, the following relationship holds:

$$P_{200}^{2/I} = \frac{1}{\Delta} \frac{\Phi_I - (\Phi_J + \Phi_K)/2}{\Phi_I + \Phi_J + \Phi_K}$$

where

$$\Delta = \frac{\alpha_2 - (\alpha_1 + \alpha_3)/2}{\alpha_1 + \alpha_2 + \alpha_3} \quad \Phi_I = \frac{n_I^2 - 1}{n_I^2 + 2}$$

and I, J and K refer to the MD, TD and ND directions.

INFLUENCE OF THE INITIAL STRUCTURE OF THE ONE-WAY DRAWN FILM ON THE DEVELOPMENT OF STRUCTURE DURING THE TRANSVERSE STRETCHING

In this section, we analyse the influence of the initial structure of the one-way drawn films on the second drawing for a second drawing temperature $T_2 = 120^\circ\text{C}$. The crystallite size along the chain axis is called the crystal length, the crystallite size along the normal to the phenylene ring is called the thickness and the crystallite size along a direction roughly perpendicular to both chain axis and the normal to the phenylene ring is called the width. A classification of samples with respect to their crystallite sizes after preheating, but before the second drawing, is shown in Table 2. In the sample notation, the first number indicates the first drawing temperature whereas the second number indicates the preheating and second drawing temperature; the length is characterized by s for short and l for long.

In Table 2, the lengths and widths of the crystallites appear to be strongly correlated for all samples: one-way drawn films have either long and wide or short and narrow crystals. The thickness is about the same for all the one-way drawn films. It is thus not possible to study the influence of the width at a given length or the influence of the length at a given width. On the other hand, it is possible to study samples that have different lengths but similar thickness. It is more difficult to study the influence

Table 2 Classification of one-way drawn films

Sample	Length		Width		Thickness		
	Short	Long	Narrow	Wide	Thin	Medium thick	Thick
$s_{103,100}$	x		x		x		
$s_{100,120}$	x		x			x	
$s_{103,120}$	x		x			x	
$s_{105,120}$	x		x			x	
$l_{100,120}$		x		x		x	
$l_{105,120}$		x		x		x	
$l_{125,120}$		x		x		x	
$l_{125,140}$		x		x			x

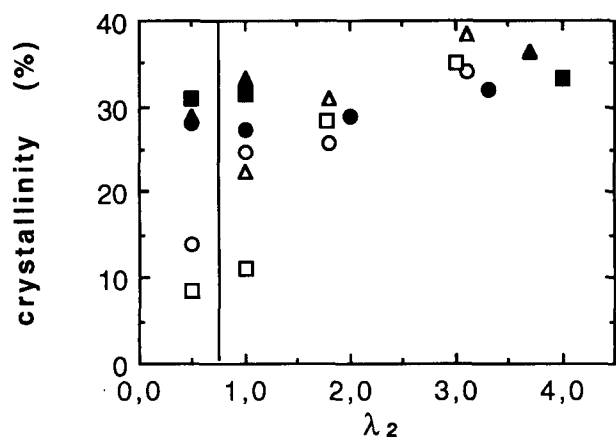


Figure 1 Crystallinity (volume fraction) versus draw ratio as a function of the morphology of the one-way drawn sample: (Δ) $s_{100,120}$; (\square) $s_{103,120}$; (\circ) $s_{105,120}$; (\blacktriangle) $l_{100,120}$; (\blacksquare) $l_{105,120}$; (\bullet) $l_{125,120}$

of the thickness at a given length, since for similar lengths of crystallites, the crystallites are either thin or of intermediate thickness or of intermediate thickness or thick.

In the following sections, to appreciate the effect of the preheating stage, the state of samples after their first drawing but before preheating will be represented on graphs at $\lambda_2 = 0.5$ for the sake of clarity, although the corresponding λ_2 is 1.0. A vertical line is drawn to separate these points from those representing actual drawn samples.

Structure of the crystalline phase

Crystallinity. The crystallinity of the various samples is plotted versus the second draw ratio in Figure 1. A strong increase in crystallinity during the preheating stage is noted for samples having initially short crystals. Samples with initially long crystals show only a slight increase of crystallinity during stretching, whereas the increase is larger for samples having initially short crystals. The crystallinity reaches a maximum value of the order of 35% at large extensions, whatever the initial structure of the films.

Orientation of the chain axes. The chain axes appear to be strongly oriented in the plane of the film, as observed previously; the value of the orientation function with respect to ND is almost constant and equal to -0.45 . From this observation, it can be concluded that any change of orientation along the machine direction will be reflected by a similar change along the transverse direction, since:

$$\sum_{j=1}^3 P_{200}^{ij} = 0$$

The X-ray diffracted intensity of the $(\bar{1}05)$ reflection is plotted in Figures 2a and 2b for two samples with long and short crystals respectively. Several qualitative observations can be made from the examination of these figures. Before preheating, the distribution of chain axes depends strongly on the length of the crystals. Films with short crystals show a rather smooth and broad distribution, whereas sharp distributions are observed in the case of large crystals. For films with short crystals, the increase in crystallinity during the preheating stage

is coupled with a sharpening of the distribution along MD. For both crystal sizes, transverse drawing leads to a broadening of the distribution of orientation of chain axes in the plane of the film, followed by the appearance of a new distribution centred along TD. Even at the largest transverse draw ratios, no sharp distribution is observed along MD or TD.

The development of the orientation with respect to the machine and transverse directions is shown quantitatively in Figures 3a and 3b. As observed previously⁵, the orientation along MD decreases and a corresponding increase of orientation occurs along the transverse direction. The original differences in P_{200} associated with differences in initial crystal size are essentially maintained; long crystals are initially more oriented along the machine direction and the initial differences remain throughout the second drawing, although the slope of the decrease of orientation with draw ratio may be slightly higher for initially short crystals.

Orientation of the ring normals. The behaviour of the crystallographic $[100]$ direction, with respect to the principal directions of the film, is shown in Figures 4a–4c. Figure 4c clearly shows that, with increasing draw ratio, the planes of the rings tend to become more oriented in the plane of the film. Differences in initial orientation with respect to ND decrease during the transverse

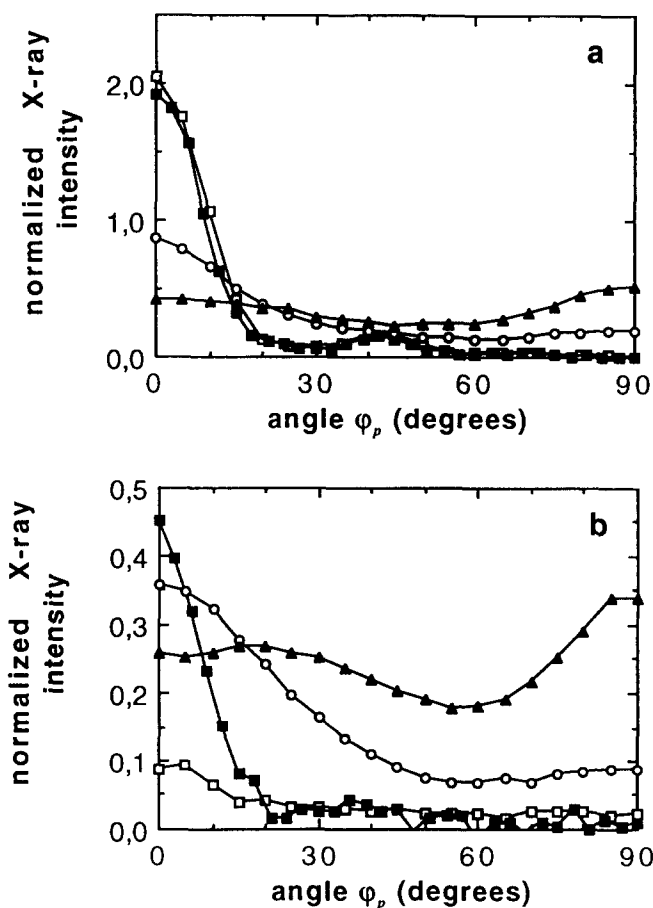


Figure 2 (a) Transmitted X-ray intensity for $(\bar{1}05)$ reflection normalized by the thickness of the sample for sample with long crystals $l_{125,120}$: (\square) one-way drawn; (\blacksquare) preheated; (\circ) $\lambda_2 = 2.7$; (\blacktriangle) $\lambda_2 = 3.8$. (b) As (a), but for sample with short crystals $s_{103,120}$: (\square) one-way drawn; (\blacksquare) preheated; (\circ) $\lambda_2 = 1.9$; (\blacktriangle) $\lambda_2 = 3.0$. The angle ϕ_p is the angle between the scattering vector and MD, with the scattering vector in the plane of the film

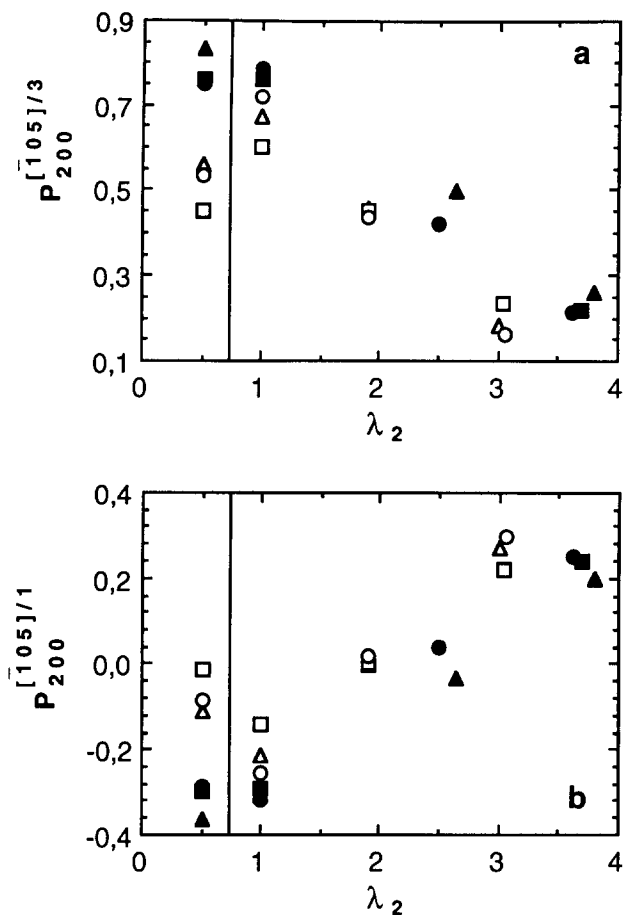


Figure 3 Orientation of the $(\bar{1}05)$ plane normal with respect to (a) the machine direction and (b) the transverse direction versus draw ratio: (Δ) $s_{100,120}$; (\square) $s_{103,120}$; (\circ) $s_{105,120}$; (\blacktriangle) $l_{100,120}$; (\blacksquare) $l_{105,120}$; (\bullet) $l_{125,120}$

stretching. However, with respect to TD (Figure 4b), samples with small crystals show a slightly greater increase in the perpendicular orientation of the $[100]$ direction.

With respect to the machine direction, as a first approximation, the orientation of the $[100]$ planes is unaffected by deformation. A more careful examination of the data shows a small loss of perpendicularity, particularly for large crystals.

Crystallite sizes. The change in crystal size along the $[100]$, $[\bar{1}05]$ and $[010]$ directions is given in Figures 5, 6 and 7 respectively. For the $[100]$ and $[\bar{1}05]$ directions, distinctions can be made as a function of the orientation of the crystals in the plane of the film. For example, depending on the orientation of the scattering vector, it is possible to measure the size of crystals that have their c axes oriented along MD or TD.

(i) L_{100} : Figure 5 shows that the thickness of the crystals increases with the second draw ratio. The slight differences observed initially do not seem to persist during the drawing: the increase in the thickness is independent of the length of crystals formed during the first drawing. The increase in thickness during this second draw is much smaller than that observed during the first drawing process.

(ii) $L_{\bar{1}05}$: Figure 6a, on the contrary, shows that, although the length of the machine-oriented crystals

decreases during drawing, the initial differences remain. In other words, on average, the number of unit cells destroyed by the second drawing is independent of the initial structure of the film. Figure 6b shows that the larger the crystals lying along the machine direction, the smaller are the newly created crystals along the transverse direction.

(iii) L_{010} : Figures 7a and 7b show the change in the width of the crystals oriented along the machine and the transverse direction respectively. For the long crystals oriented along MD, the width clearly decreases during stretching. For short crystals, this dimension remains fairly constant. It can be seen from Figure 7b that the width of the crystals created along TD increases strongly

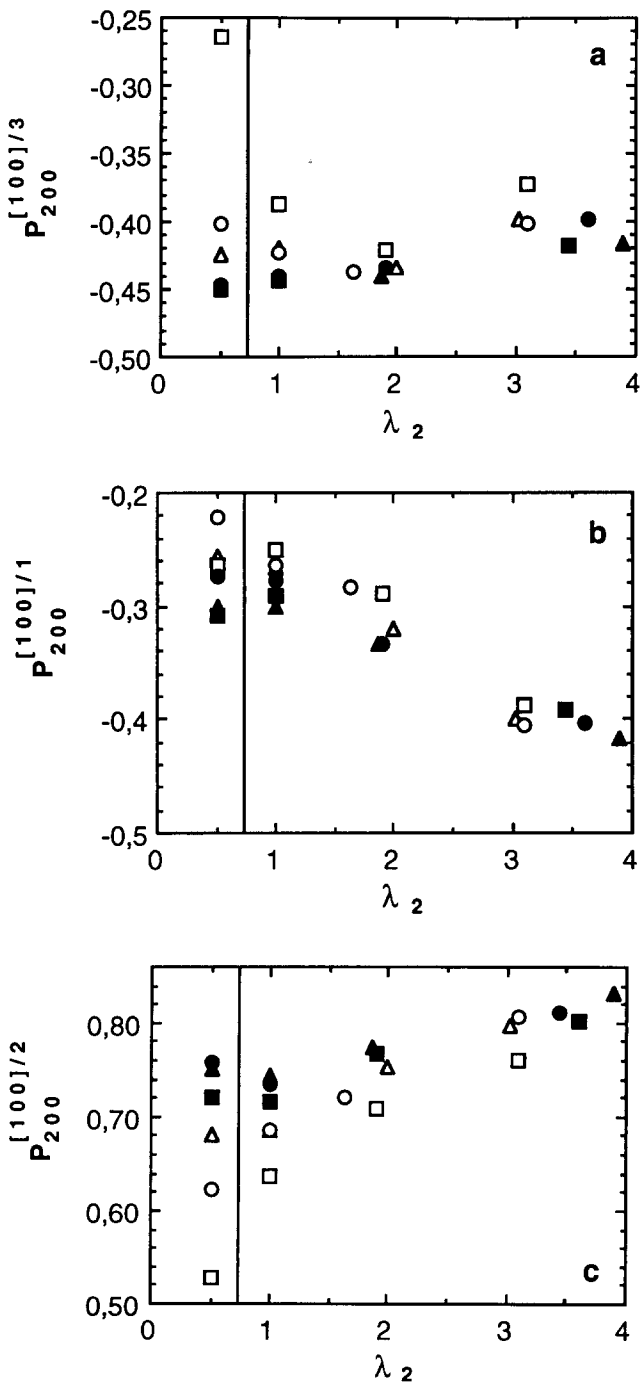


Figure 4 Orientation of the (100) plane normal with respect to (a) the machine direction, (b) the transverse direction and (c) the normal direction versus draw ratio: (Δ) $s_{100,120}$; (\square) $s_{103,120}$; (\circ) $s_{105,120}$; (\blacktriangle) $l_{100,120}$; (\blacksquare) $l_{105,120}$; (\bullet) $l_{125,120}$

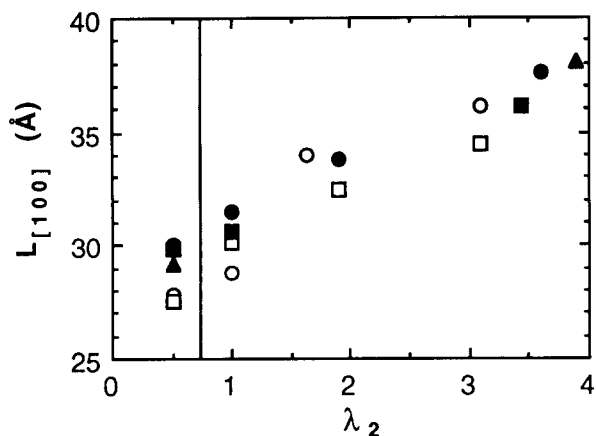


Figure 5 Evolution of the thickness of the crystals during transverse stretching: (Δ) $s_{100,120}$; (\square) $s_{103,120}$; (\circ) $s_{105,120}$; (\blacktriangle) $l_{100,120}$; (\blacksquare) $l_{105,120}$; (\bullet) $l_{125,120}$

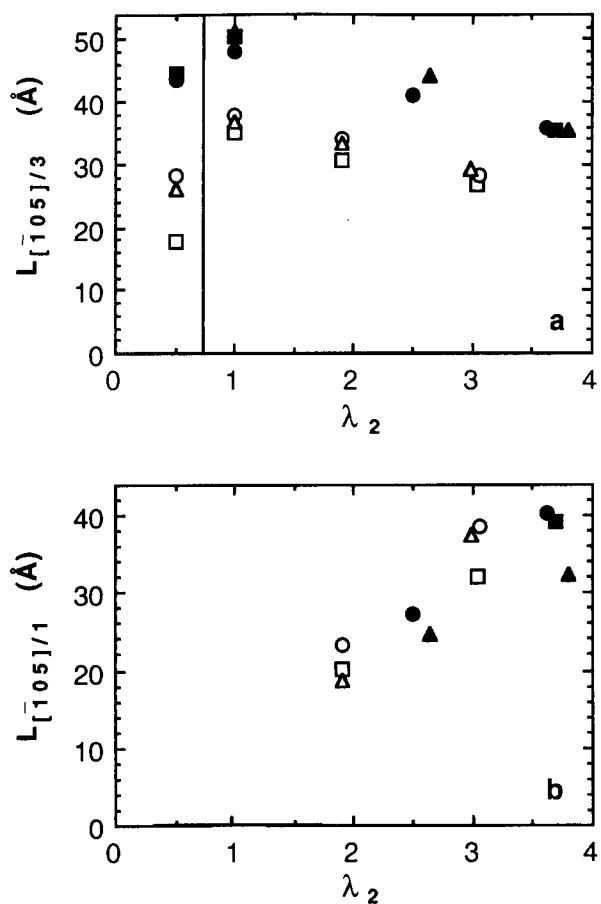


Figure 6 Evolution of the length of the crystals for (a) crystals oriented parallel to MD and (b) crystals oriented parallel to TD versus draw ratio: (Δ) $s_{100,120}$; (\square) $s_{103,120}$; (\circ) $s_{105,120}$; (\blacktriangle) $l_{100,120}$; (\blacksquare) $l_{105,120}$; (\bullet) $l_{125,120}$

with the deformation. There seems to be a strong correlation between the increase of the lengths of crystals oriented along TD (as seen in Figure 6b) and the increase in their corresponding widths (Figure 7b). However, this is not true for the remaining crystals aligned along MD. Although their length is decreasing, no decrease of their width is observed, especially for initially short crystals. This may indicate different types of deformation mechanisms for films containing long or short crystals.

Overall orientation as measured by birefringence

Orientation of the normal to the phenylene ring. The overall orientation of the normal to the phenylene ring is shown in Figures 8a–8c. In all these figures, the level of orientation is lower than that observed for the [1 0 0] direction in the crystalline phase: this may be attributed to the contribution of the amorphous phase, which is less oriented than the crystalline phase.

Figure 8a shows that during drawing, on average, the normals to the phenylene rings become less perpendicularly oriented with respect to the machine direction, in contrast to the crystalline phase alone, where the normals remain strongly perpendicular to MD. This phenomenon, which can be qualitatively attributed to the amorphous phase, is more pronounced for samples containing initially long crystals.

Figures 8b and 8c show, however, that overall the normals to the phenylene rings tend to become oriented away from the transverse direction and towards the normal direction. The reorientation towards the normal direction produces a greater change in the corresponding P_{200} than that observed for the ring normals in the crystalline phase (compare Figures 4c and 8c). This is because the crystalline (1 0 0) planes are so highly oriented parallel to the plane of the film during the first draw that reorientation of the chain axes and rotation around them can produce little further orientation of the ring planes; it can, however, increase the orientation for

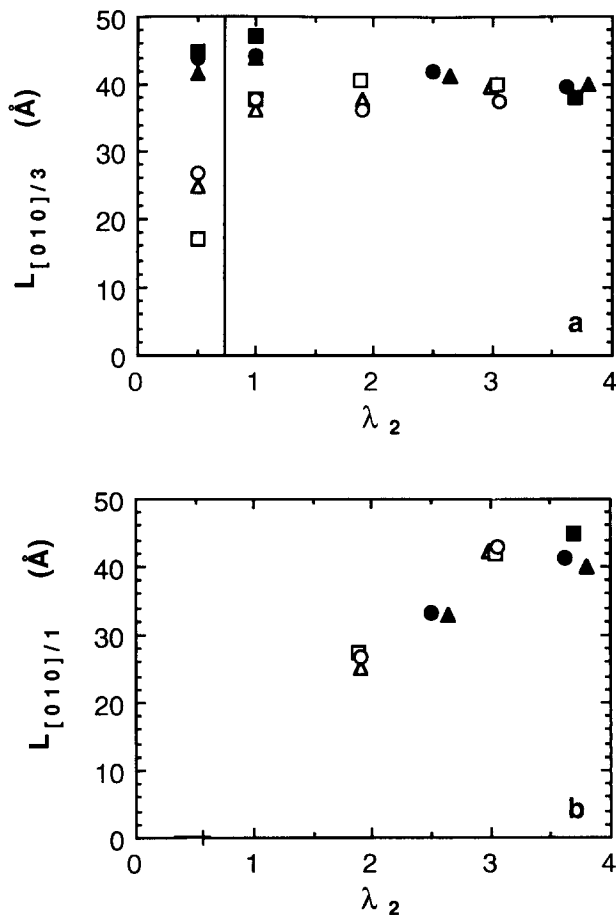


Figure 7 Evolution of the width of the crystals for (a) crystals oriented parallel to MD and (b) crystals oriented parallel to TD versus draw ratio: (Δ) $s_{100,120}$; (\square) $s_{103,120}$; (\circ) $s_{105,120}$; (\blacktriangle) $l_{100,120}$; (\blacksquare) $l_{105,120}$; (\bullet) $l_{125,120}$

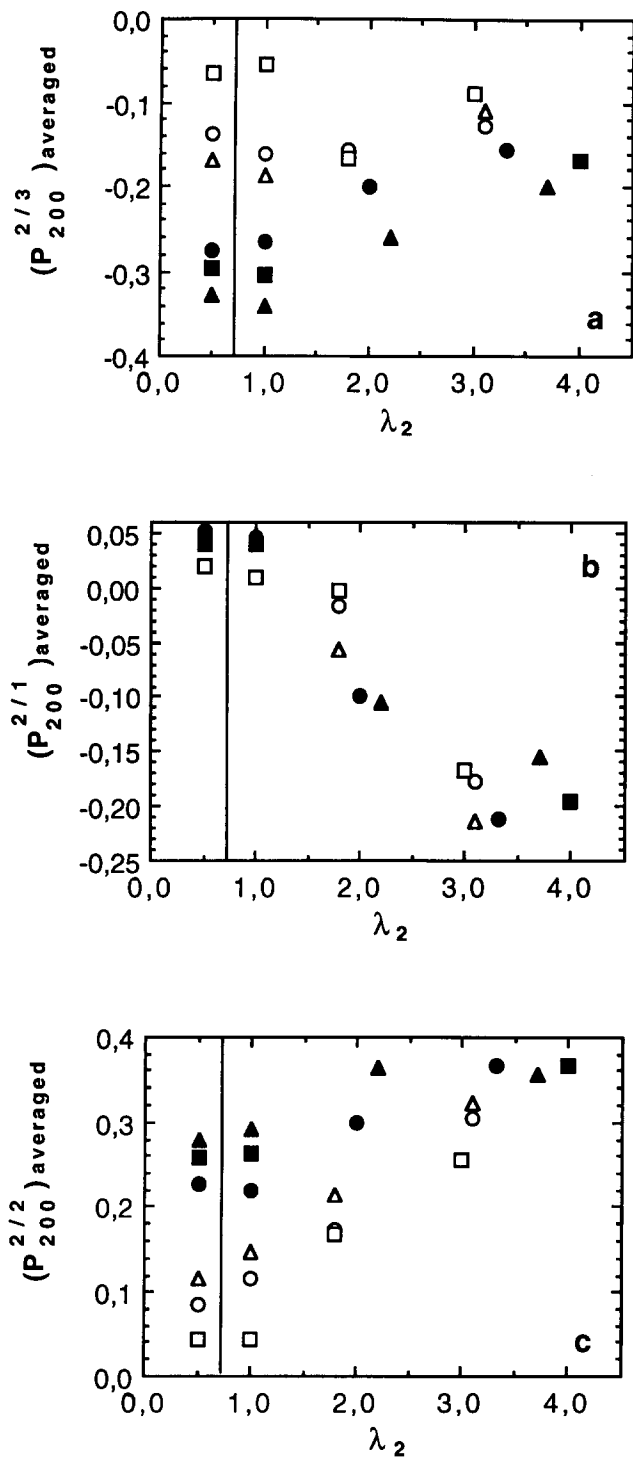


Figure 8 Orientation of the normal to the phenyl ring averaged over the amorphous and crystalline phases versus draw ratio, (a) with respect to MD, (b) with respect to TD and (c) with respect to ND: (Δ) $s_{100,120}$; (\square) $s_{103,120}$; (\circ) $s_{105,120}$; (\blacktriangle) $l_{100,120}$; (\blacksquare) $l_{105,120}$; (\bullet) $l_{125,120}$

the rings of chains in the amorphous phase (compare also *Figures 4b* and *8b* and *Figures 4a* and *8a*).

The increase in orientation towards the normal to the film is higher for samples having small crystals, reflecting the trends observed in the crystalline phase. However, even at large draw ratios, the phenylene rings (on average over the material) are less oriented in the plane of the film for samples having initially small crystals, whereas, in the crystalline phase, almost the same level of orientation is obtained.

INFLUENCE OF THE SECOND DRAWING TEMPERATURE ON THE STRUCTURE OF THE FILM

Description of the crystalline phase

Crystallinity. The changes in crystallinity during the second drawing are shown in *Figure 9*. As stated above, the increase in crystallinity is much more marked for films having initially short crystals than for those having initially long crystals.

The maximum level of crystallinity (obtained for $\lambda_2 > 3$) correlates strongly with the second drawing temperature. The maximum is at 25% for $T_2 = 100^\circ\text{C}$, about 35% at $T_2 = 120^\circ\text{C}$ and 40% at $T_2 = 140^\circ\text{C}$. Since the degree of crystallinity is strongly dependent on the draw temperature, the morphology of the crystals will be described before the molecular orientation.

Crystallite sizes.

(i) L_{105} : The changes in length along the $[\bar{1}05]$ direction are shown in *Figures 10a* and *10b* for crystals oriented along MD and TD respectively. Clearly, the preheating step has a great influence, especially for short crystals.

The stretching temperature does not affect the decrease of length along the machine direction for samples having small crystals. In the case of initially long crystals, an increase of temperature leads to a slightly smaller decrease in size along this direction. Overall, however, the initial differences in size are retained.

On the contrary, along the transverse direction, stress-induced crystals show a length that increases with the draw temperature, as might be expected from thermodynamic crystal growth considerations.

(ii) L_{010} : *Figure 11a* shows the changes in width of the crystals oriented along the machine direction and *Figure 11b* the changes along the transverse direction. For the initially long crystals, their width decreases slightly during stretching, especially at 140°C . Short crystals maintain this dimension rather stably during stretching, whatever the temperature. It can be seen from *Figure 11b* that the width of the crystals created with their c axes parallel to X_1 increases strongly with the deformation and also with increasing draw temperature, especially at high draw temperatures.

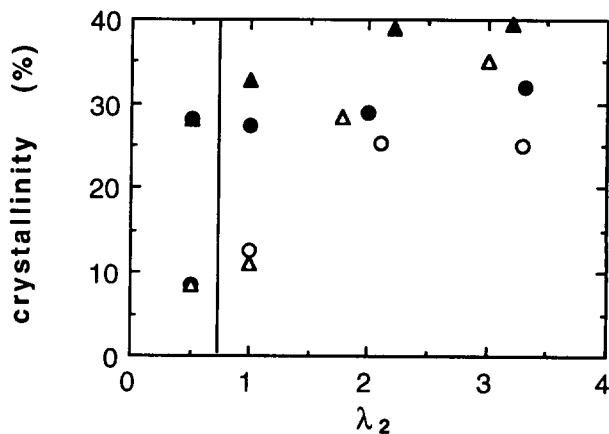


Figure 9 Crystallinity (volume fraction) versus draw ratio as a function of the morphology of the one-way drawn sample for different transverse stretching temperatures: (\circ) $s_{103,100}$; (Δ) $s_{103,120}$; (\bullet) $l_{125,120}$; (\blacktriangle) $l_{125,140}$

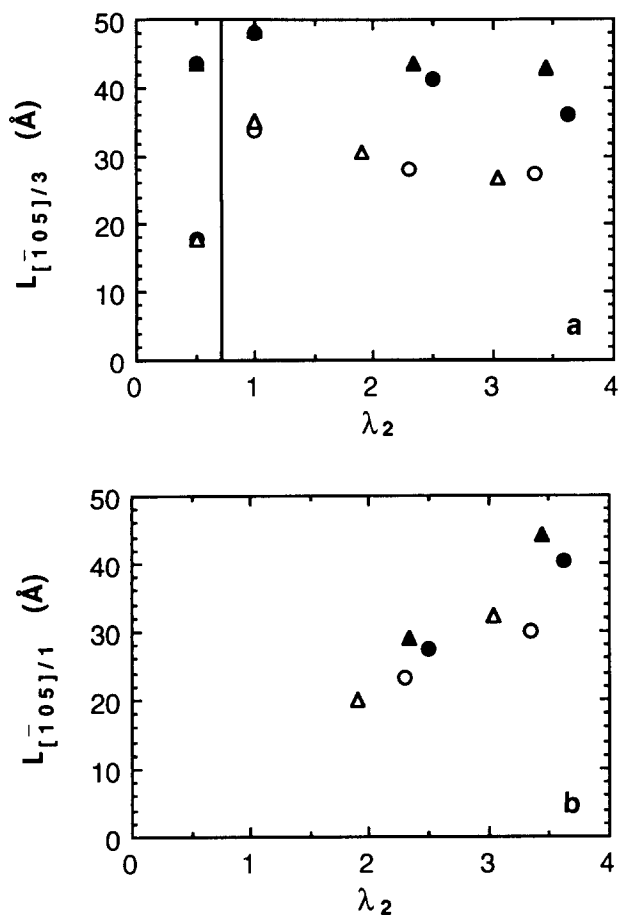


Figure 10 Evolution of the length of the crystals for (a) crystals oriented parallel to MD and (b) crystals oriented parallel to TD versus draw ratio for different temperatures and samples: (○) $s_{103,100}$; (△) $s_{103,120}$; (●) $l_{125,120}$; (▲) $l_{125,140}$

(iii) L_{100} : The thickness of the crystals clearly increases with draw temperature (Figure 12). At low draw temperatures (100°C), the thickness of the crystals is independent of the draw ratio. At higher temperatures, an increase in the thickness is observed.

Orientation

Chain axes. The orientation of the chain axes is shown in Figures 13a and 13b. Long crystals show a higher degree of orientation along the machine direction at higher draw temperatures. For small crystals, it appears more difficult to draw definite conclusions. Nevertheless, it appears that the initial differences in orientation observed for the small crystals at different temperatures reduce as the draw ratio is increased.

Normal to the ring. The orientation of the (1 0 0) planes with respect to the principal directions is given in Figures 14a–14c. The influence of temperature seems to be much lower than that of the initial size of the crystals. No temperature effect can be discerned for small crystals. As far as large crystals are concerned, an increase in draw temperature acts in favour of a slightly more pronounced orientation of the ring plane in the plane of the film and a more perpendicular orientation with respect to the machine direction.

We may note that the behaviour of the (1 0 0) planes is fully compatible with that of the chain axes. Since the

chain axes have a greater tendency to keep their orientation along the machine direction as the draw temperature increases, the normal to the rings tends to be more perpendicular to the machine direction. For small crystals, no effect of draw temperature can be discerned on either the [1 0 0] or the $[\bar{1} 0 5]$ directions.

Average orientation as measured by birefringence

Orientation of the normal to the phenylene ring. The orientation of the ring normals is shown in Figures

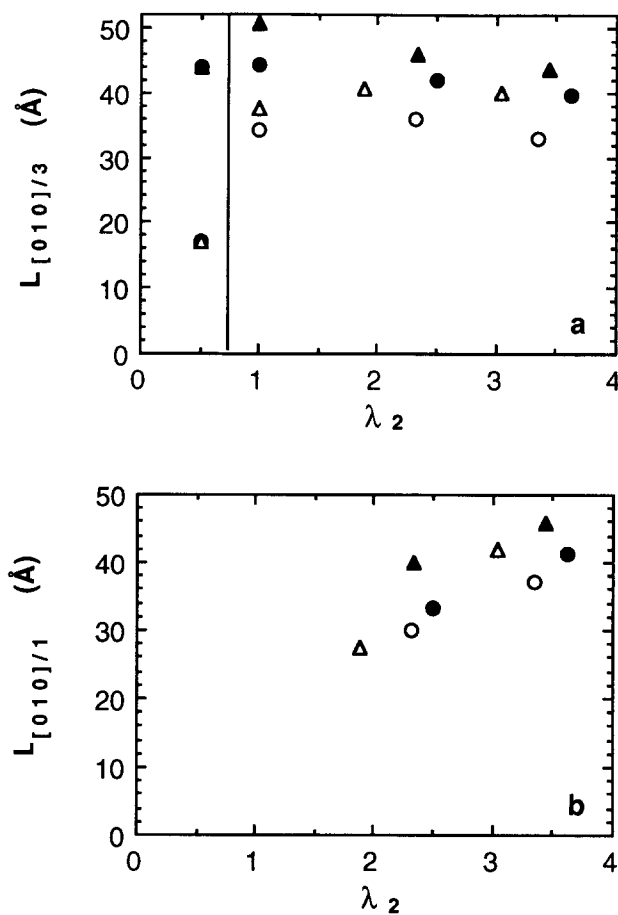


Figure 11 Evolution of the width of the crystals for (a) crystals oriented parallel to MD and (b) crystals oriented parallel to TD versus draw ratio for different temperatures and samples: (○) $s_{103,100}$; (△) $s_{103,120}$; (●) $l_{125,120}$; (▲) $l_{125,140}$

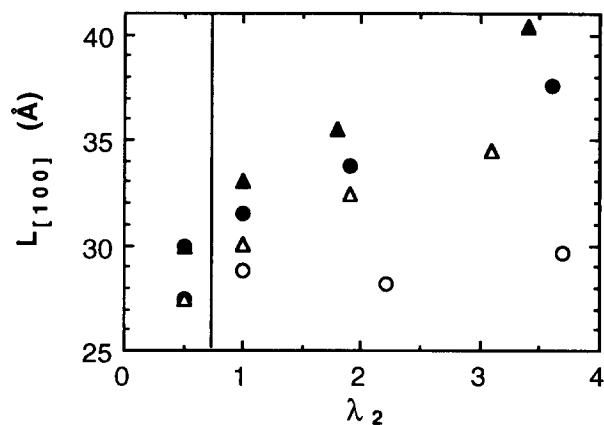


Figure 12 Evolution of the thickness of the crystals versus draw ratio for different temperatures and samples: (○) $s_{103,100}$; (△) $s_{103,120}$; (●) $l_{125,120}$; (▲) $l_{125,140}$

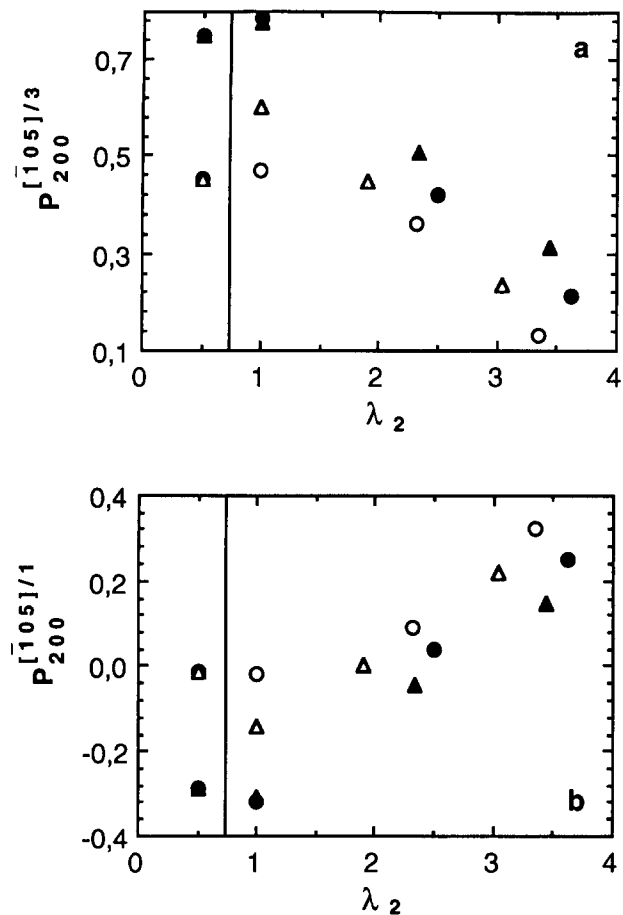


Figure 13 Orientation of the (105) plane normal with respect to (a) the machine direction and (b) the transverse direction versus draw ratio for various temperatures and samples: (○) $s_{103,100}$; (△) $s_{103,120}$; (●) $l_{125,120}$; (▲) $l_{125,140}$

15a–15c. For films with long crystals the loss of perpendicularity of the ring normal with respect to the machine direction (Figure 15a) or the tendency of the ring plane to orient in the plane of the film (Figure 15c) are almost independent of temperature. On the other hand, for films with short crystals, it can be seen from Figure 15c that the tendency of the ring planes to orient in the plane of the film, as the transverse drawing proceeds, is lower at low temperatures. For the crystalline phase, very little influence of the temperature was observed. This means that the temperature is mainly affecting the tendency of the rings in the amorphous phase to orient parallel to the plane of the film.

The increase in perpendicularity of the ring normals with respect to the transverse direction does not seem to be strongly affected by the temperature whatever the initial size of the crystals, as was also observed for the crystalline phase, except at 100°C, where the reorientation appears to be more difficult.

DISCUSSION

In this section, the most interesting features of the second drawing process will be emphasized and discussed.

Preheating stage

The preheating stage, which is similar to that in the industrial process, has a strong influence on the structure

of the films, especially those produced from samples having short crystals at the end of the first drawing stage. An increase in the size of the crystals is observed, together with an increase of the orientation along the machine direction.

This result can be explained by the fact that films with short crystals are essentially 'quenched' samples, i.e. in a non-equilibrium state. During thermal treatment, crystallization occurs in order to reach the equilibrium crystallinity. Since the sample remains dimensionally constrained during preheating, almost no relaxation occurs and stretched chains may crystallize. The increase in the crystal size suggests that only a growth

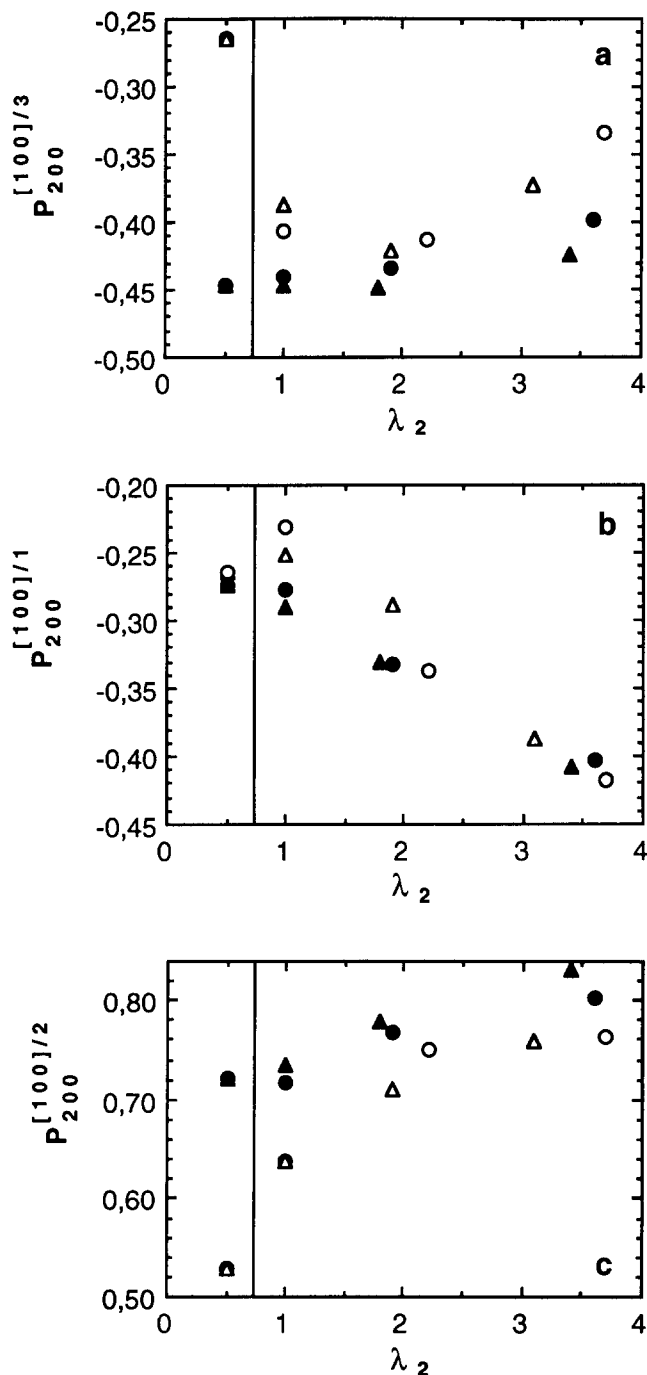


Figure 14 Orientation of the (100) plane normal with respect to (a) the machine direction, (b) the transverse direction and (c) the normal direction versus draw ratio: (○) $s_{103,100}$; (△) $s_{103,120}$; (●) $l_{125,120}$; (▲) $l_{125,140}$

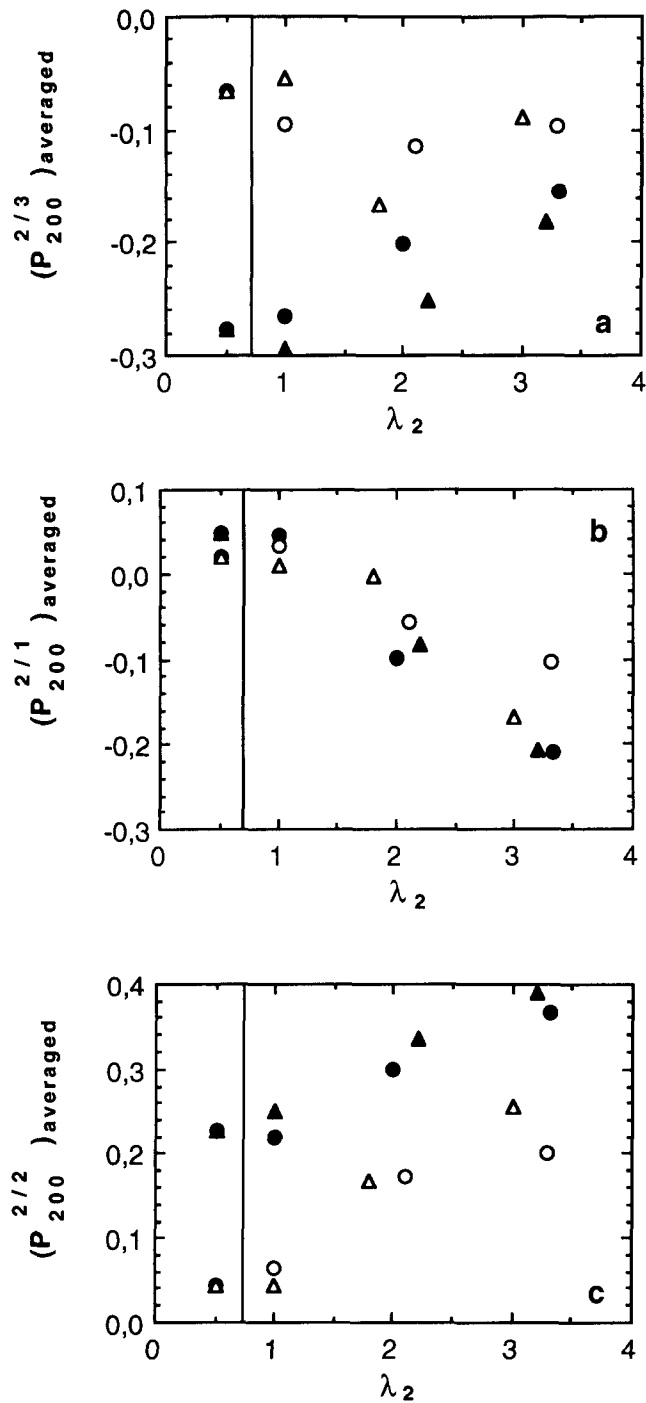


Figure 15 Orientation of the normal to the phenyl ring averaged over the amorphous and crystalline phases versus draw ratio, (a) with respect to MD, (b) with respect to TD and (c) with respect to ND, for various temperatures and samples: (○) $s_{103,100}$; (△) $s_{103,120}$; (●) $l_{125,120}$; (▲) $l_{125,140}$

phenomenon is observed. The growth process is more pronounced as the preheating temperature is increased, as expected from kinetic considerations.

Growth in crystal size and orientation during transverse stretching

Irrespective of the size of the crystals in the initial one-way drawn film, the same orientation behaviour is observed during transverse stretching and the crystalline phase exhibits a biaxial structure. Transverse drawing leads to progressive destruction of the initial machine-

oriented crystalline structure, with the formation of a new, transversely oriented, crystalline structure. A qualitative correlation is observed between the growth of the crystalline structure oriented along the transverse direction and the increase of orientation in this direction.

The growth of the crystals oriented along the transverse direction appears easier when short crystals are present initially. This observation can be correlated with the fact that at all draw ratios a higher level of orientation is observed with respect to the transverse direction for the samples that initially had shorter crystals. Qualitatively, this behaviour can be explained by the fact that in films containing small crystals, a lower crystallinity is observed, so that chains are able to orient in a less constrained environment.

Support for this proposition is given by the results for the crystal size along the $[\bar{1}05]$ direction for the crystals oriented at 45° with respect to MD or TD. Initially (after preheating), no diffracted X-ray intensity can be measured in this direction. During transverse stretching, broadening of the signal along MD generates a diffracted signal around 45° . The length of the crystals in this direction is plotted versus the draw ratio in Figure 16 for samples having long or short crystals. It appears that the smaller the initial crystals, the longer are the crystals oriented at intermediate angles. Furthermore, an increase in crystal size is observed as the transverse draw ratio increases. If we assume that these structures originate from the breakage of larger blocks that were initially oriented along MD, it appears that breakage and rotation of these structures is easier in films containing initially short crystallites. These structures orient during transverse stretching along TD and may act as nuclei to promote orientation-induced crystallization along TD. The easier rotation of small structures in less constrained surroundings may explain the higher level of orientation along TD and more rapid growth of crystals observed in films with short crystals.

The difference between the change in width of the crystals oriented along MD for long or short structures indicates that there may be a different mechanism operating. In the case of long crystals, we have seen that breakage and rotation of MD-oriented blocks is difficult and, correspondingly, a decrease of the width is observed, which can be attributed to an additional peeling mechanism. Such a mechanism does not seem to be

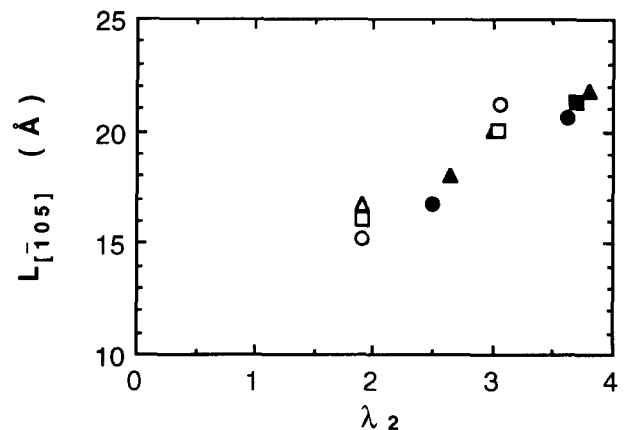


Figure 16 Size along direction $[\bar{1}05]$ of the crystals oriented at 45° in the plane of the film for various samples: (△) $s_{100,120}$; (□) $s_{103,120}$; (○) $s_{105,120}$; (▲) $l_{100,120}$; (■) $l_{105,120}$; (●) $l_{125,120}$

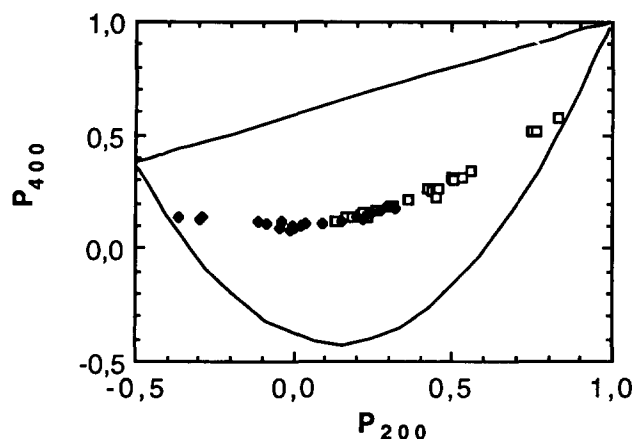


Figure 17 Relationship between P_{200} and P_{400} for samples investigated in this study: (\square) $P_{400}^{[T05]/3}$ versus $P_{200}^{[T05]/3}$; (\blacklozenge) $P_{400}^{[T05]/1}$ versus $P_{200}^{[T05]/1}$

relevant for short crystals that can more easily break down and rotate.

Influence of draw temperature during transverse stretching

The influence of the draw temperature during transverse stretching can be understood as the result of competition between two processes, molecular relaxation and crystallization. Low stretching temperatures imply slow relaxation processes and low mobility, leading to slow crystallization kinetics; reorientation and breakdown of crystals is difficult owing to low molecular mobility. Reorientation of the amorphous phase is also difficult at low temperatures, as seen in Figure 15. Conversely, at elevated temperatures, the molecular mobility is higher and the tendency of the chains to crystallize during orientation is greater. Larger crystals are therefore created at such temperatures (Figure 10). However, reorientation of the one-way drawn film is difficult because it is restricted by the strong tendency of the chains to crystallize. In fact, it appears that there is an optimum temperature of around 120°C, where the molecular mobility is sufficient to allow rotation of small crystalline units, but low enough to avoid rapid crystallization.

P_{200} vs. P_{400} relationship

The description of the orientation distribution function by the P_{200} data alone is clearly inadequate and further information can be obtained if the P_{400} values can be determined. In the case of the crystalline phase, the X-ray diffraction data directly reflect the distribution function and P_{400} values can be calculated by a procedure almost identical to that used for P_{200} . It is known that, for a given value of P_{200} , P_{400} can vary between two limits corresponding (in the case of uniaxial distribution) to a

bimodal distribution along MD and TD or a unimodal distribution, but located at a specific angle. In Figure 17, the P_{400} values corresponding to our samples have been plotted versus the corresponding P_{200} values. It is interesting to note that all the points cluster along a 'master curve'. This suggests that the shape of the orientation distribution function is entirely controlled by the second moment P_{200} and not by the size of the crystals. At intermediate values of P_{200} , a necessarily smooth, somewhat bimodal distribution is observed.

CONCLUSIONS

This study of changes in orientation and crystal size during the transverse drawing of initially one-way drawn PET films provides new information about the mechanisms involved in this deformation process. Whatever the initial structure of the one-way drawn films, the development of biaxial orientation proceeds by a loss of orientation along the machine direction and the creation of an oriented structure along the transverse direction. However, the detailed mechanisms depend on the size of the crystals present. Small crystals lead to biaxially oriented films at transverse draw ratios lower than those for films containing long crystals that are difficult to reorient and for which the growth of the transverse structure is clearly slower. The second drawing temperature can be chosen to optimize the biaxial orientation process.

ACKNOWLEDGEMENTS

We would like to thank Professor L. Monnerie and Dr P. Lapersonne for fruitful discussions. We also gratefully acknowledge Rhône-Poulenc Films for providing a PhD Fellowship for one of us (J.B.F.).

REFERENCES

- 1 Lapersonne, P., Tassin, J. F., Monnerie, L. and Beutemps, J. *Polymer* 1991, **32**, 3331
- 2 Lapersonne, P., Bower, D. I. and Ward, I. M. *Polymer* 1992, **33**, 1266
- 3 Lapersonne, P., Bower, D. I. and Ward, I. M. *Polymer* 1992, **33**, 1277
- 4 Lapersonne, P., Tassin, J. F. and Monnerie, L. *Polymer* 1994, **35**, 2192
- 5 Faisant de Champchesnel, J. B., Bower, D. I., Ward, I. M., Tassin, J. F. and Lorentz, G. *Polymer* 1993, **34**, 3763
- 6 Lebourvellec, G., Jarry, J. P. and Beutemps, J. *J. Appl. Polym. Sci.* 1990, **39**, 319
- 7 Lebourvellec, G. and Beutemps, J. *J. Appl. Polym. Sci.* 1990, **39**, 329
- 8 Lapersonne, P., Thèse de Doctorat, Université P. et M. Curie, Paris, 1991
- 9 Ward, I. M. *Adv. Polym. Sci.* 1985, **66**, 81
- 10 De Vries, A. J., Bonnebat, C. and Beutemps, J. *J. Polym. Sci.* 1977, **58**, 109
- 11 Daubeny, R., Bunn, C. W. and Brown, C. J. *Proc. R. Soc. (A)* 1954, **226**, 531
- 12 Jarvis, D. A., Hutchinson, I. J., Bower, D. I. and Ward, I. M. *Polymer* 1980, **21**, 41